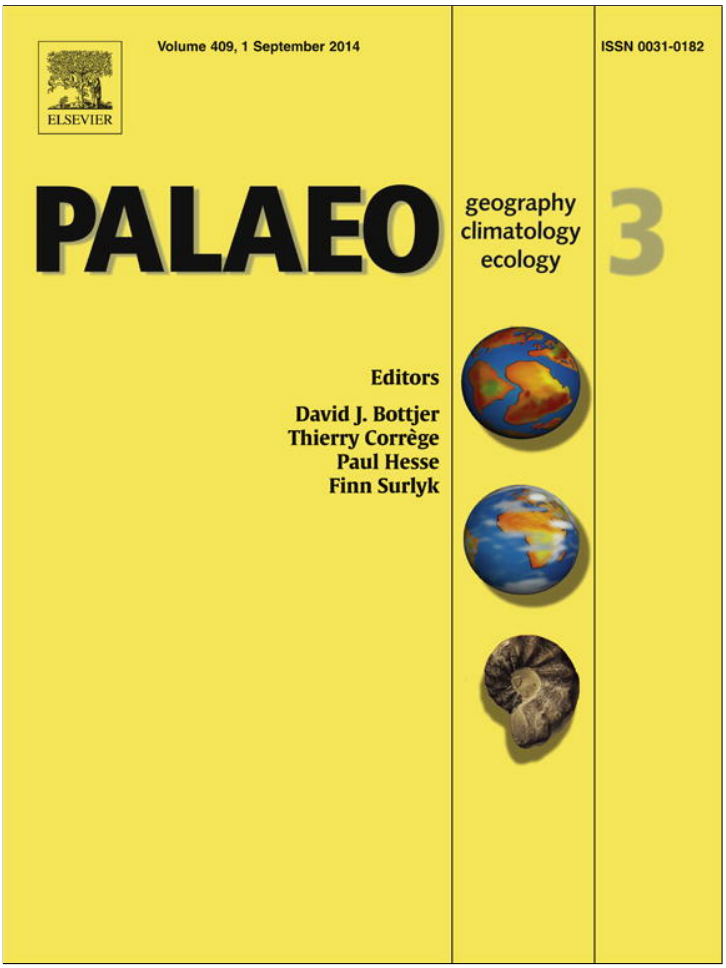

Palaeogeography, Palaeoclimatology, Palaeoecology 409 (2014) 1–8

Contents lists available at ScienceDirect

Palaeogeography, Palaeoclimatology, Palaeoecology

journal homepage: www.elsevier.com/locate/palaeo

# Characterization of the last deglacial transition in tropical East Africa: Insights from Lake Albert

Melissa A. Berke [a,b,*,1], Thomas C. Johnson [a,b], Josef P. Werne [c], Daniel A. Livingstone [d], Kliti Grice [e], Stefan Schouten [f], Jaap S. Sinninghe Damsté [f]

[a] Large Lakes Observatory, University of Minnesota Duluth, Duluth, MN 55812, USA
[b] Dept. of Geological Sciences, University of Minnesota Duluth, Duluth, MN 55812, USA
[c] Dept. of Geology & Planetary Science, University of Pittsburgh, Pittsburgh, PA 15260, USA
[d] Dept. of Biology, Duke University, Durham, NC 27708, USA
[e] WA-Organic and Isotopic Geochemistry Centre, Dept. of Chemistry, Curtin University, Perth, Australia
[f] NIOZ Royal Netherlands Institute for Sea Research, Dept. of Marine Organic Biogeochemistry, The Netherlands

ARTICLE INFO

*Article history:*
Received 23 November 2013
Received in revised form 18 April 2014
Accepted 27 April 2014
Available online 10 May 2014

*Keywords:*
African paleoclimate
Sedimentary molecular biomarkers
$TEX_{86}$ paleotemperature
Compound specific carbon and hydrogen isotopes
Lake Albert
Deglaciation

ABSTRACT

New biomarker analyses from Lake Albert, East Africa spanning ~15–9 ka show the most extreme, abrupt, multi-stage climate and environmental shifts during the last deglacial transition of anywhere in Africa. Records of hydroclimate expressed in compound specific δD values from terrestrial leaf waxes and a $TEX_{86}$ paleotemperature record support multiple stages of pronounced drying and cooling from 13.8 to 11.5 ka and demonstrate the dynamic behavior of the low latitude tropics during the deglaciation. The vegetation response, illustrated by compound specific $\delta^{13}C$ values and fossil pollen records, was an expansion of $C_4$ grassland when the region was cool and arid. These results advance our understanding of a spatially and temporally complex regional response to global climate forcing, suggesting weakening of the Indian Ocean monsoon at the end of the Pleistocene that coincides with a minor decrease in the rate of the Atlantic Meridional Overturning Circulation (AMOC) and during a time of stepwise cooling in the northern high latitudes.



## 1. Introduction

Debate regarding the history of millennial scale climate variability in the African tropics includes the geographic extent, synchroneity of onset and termination, and potential forcing mechanisms associated with the global deglaciation. Difficulty in constraining the response and causal mechanisms during these intervals is associated with the seemingly abrupt, short-lived nature of events that involve nonlinear and complex feedbacks. Commonly defined from the Greenland ice cores, the 'deglacial transition' contains the Bølling/Allerød (BA), a warm, wet interstadial period, beginning ~14.7 ka and ending with the start of the Younger Dryas (YD) at ~12.7 ka (Alley and Clark, 1999), marked by pronounced cooling. The BA is punctuated by three abrupt, century-scale cold events: the intra-Bølling, the Older Dryas (OD), and the intra-Allerød (Alley and Clark, 1999). Near this time, the Southern Hemisphere also underwent a cold interval called the Antarctic Climate Reversal (ACR), ~14.8–12 ka (Jouzel et al., 1995). Records from the Northern and Southern hemispheres, specifically the high latitude polar regions, suggest an anti-phased climate response during the deglacial that has been termed the 'bipolar seesaw'(Broecker, 1998; Alley and Clark, 1999). These intervals are commonly attributed to a variety of mechanisms that include changes to oceanic circulation, atmospheric greenhouse gases, ice sheet extent, and orbital insolation (Alley and Clark, 1999). A statistical synthesis of global records that span the deglaciation characterized a first mode of variability related to rising $CO_2$, and a second mode that reflects the bipolar seesaw effects of the Atlantic Meridional Overturning Circulation (AMOC) (Shakun and Carlson, 2010).

The East African expression of these millennial-scale perturbations in climate during the shift from a relatively arid Last Glacial Maximum (LGM) to a wetter early Holocene (Gasse, 2000) is complex and is an ongoing area of research. This is in part due to the orographic complexity of East Africa, to shifting boundaries between major air masses, and to changing patterns of sea surface temperature in the Indian and Atlantic Oceans that can affect the timing and response to global and regional triggers. Paleorecords suggest both spatially uniform and variable African climate responses to perturbations during the last deglaciation. For instance, there is evidence of extensive aridity

* Corresponding author at: 156 Fitzpatrick Hall, University of Notre Dame, Notre Dame, IN 46556, USA. Tel.: +1 574 631 4857.
*E-mail address:* mberke@nd.edu (M.A. Berke).
[1] Current address: Dept. of Civil & Environmental Engineering & Earth Sciences, University of Notre Dame, Notre Dame, IN 46556, USA.

http://dx.doi.org/10.1016/j.palaeo.2014.04.014
0031-0182/

in tropical Africa contemporaneous with the YD, including decreased lake levels and river discharge and changes in wind regime (Talbot et al., 2007 and references therein). However, the interval immediately preceding the YD, a time when the Greenland ice core $\delta^{18}O$ records demonstrate a pronounced, step-wise cooling in the Northern high latitudes, shows a more spatially and temporally heterogeneous pattern of African climate response. Our understanding of this time period in Africa is far from complete.

In this study, we focus on the climate dynamics of the equatorial tropics around Lake Albert, specifically addressing the question of whether this region responded in a congruent way with other African records. We present new biomarker records from Lake Albert comparing $TEX_{86}$ paleotemperatures and compound specific $\delta^{13}C$ and $\delta D$ values of leaf waxes to provide records of temperature, vegetation change, and hydroclimate, respectively. These records indicate that the region surrounding Lake Albert underwent a multi-stage climatic and environmental shift after the LGM not seen everywhere across Africa.

## 2. Methods & background

Lake Albert lies at 2° N in the Rift Valley between Uganda and the Democratic Republic of the Congo at an altitude of 620 m (Fig. 1). The region today receives rain in two seasons: August–November and March–May (Nicholson, 1996), linked to the position and intensity of the Intertropical Convergence Zone (ITCZ). The Congo Air Boundary (CAB) is also nearby, marking the convergence of moisture derived from the Atlantic and Indian Oceans.

We analyzed sediment from Core F, collected in Lake Albert in 1971 (1°50.1′N, 31°10.2′E, 46 m water depth) by Prof. Dan Livingstone and his student, Thomas Harvey, of Duke University (Harvey, 1976). The upper 6.6 m of core consisted of dark gray–black diatomaceous mud overlying a thin sand layer. Between 6.6 and 8.4 m, the lithology changes dramatically into partially lithified sediments indicating frequent desiccation with few to no diatoms and ostracods but abundant root traces. The basal 80 cm of the core (8.4–9.2 m burial depth) consists of laminated black muds with visible diatoms and sponge spicules, interpreted to signify a shallow, well-mixed lake (Beuning et al., 1997). The top 1 m of core originally contained finely laminated muds, but these had been heavily sampled prior to this study.

We use a previously established age model based on 11 radiocarbon dates, 7 from Core F and 4 from core G (another core taken at the same site), correlated lithologically with Core F (Fig. 1, Table 1) (Beuning et al., 1997; Williams et al., 2006). Six of the eleven dates define a nearly constant sedimentation rate of about 1.0 m/ky that spans the interval in this paper, from 12,500 ± 190 $^{14}C$ ybp (14.76 ± 0.44 ka) at 640–665 cm depth in core (which lies just above a paleosol representing the Late Pleistocene desiccation of Lake Albert as described above (Beuning et al., 1997) to 8230 ± 60 $^{14}C$ ybp (9.21 ± 0.10 ka) at 84 cm depth in core. The core was sampled where intact, from 71 to 606 cm, corresponding to ~7.1–14.3 ka, with an average sampling interval of 15 cm, corresponding to ~150 years. Absolute age uncertainty within this sampled interval is about 200 years.

### 2.1. Sedimentary biomarker extraction and purification

Freeze-dried, homogenized sediments (typically 1–3 g dry weight) were extracted using soxhlet extraction with 2:1 DCM:MeOH for 24 h to produce a total lipid extract (TLE). The TLE was isolated into neutral, free fatty acid, and phospholipid fatty acid fractions using an aminopropylsilyl bond elute column, cleaned prior to use. Short column chromatography with activated alumina as the stationary

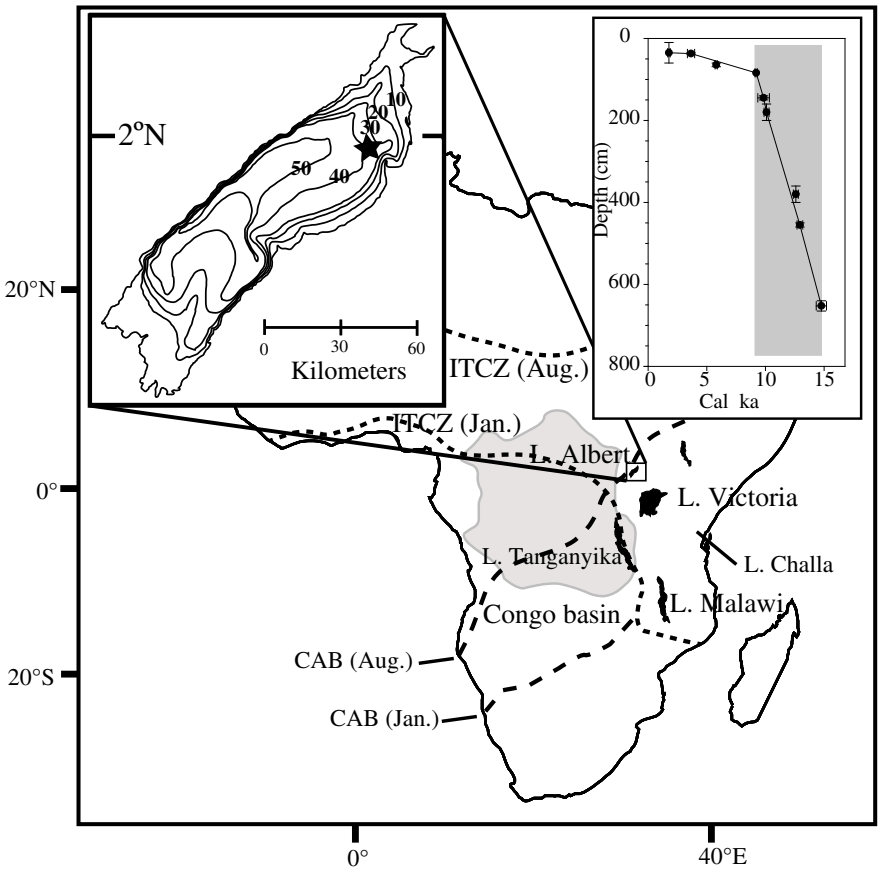


**Fig. 1.** Map of Lake Albert (star) and Lakes Malawi, Tanganyika, Victoria, Challa, and the Congo Basin. Inset: Chronology of Lake Albert Core F. The shaded section indicates the interval sampled for this study.

**Table 1**
Core chronology for the uppermost 7 m of Lake Albert Core F (Beuning et al., 1997; Williams et al., 2006). Horizontal (radiocarbon) and vertical (sampled sediment range) error bars shown. Core G dates (sampled from another core at the same site) indicated with (G) next to the depth range.

| Depth (cm) range | $^{14}$C years BP | Cal ybp | Material |
|---|---|---|---|
| 10–60 | 1850 ± 90 | 1777 ± 107 | Bulk organic matter |
| 35–39 | 3370 ± 250 | 3656 ± 310 | Bulk organic matter |
| 64.5 | 5050 ± 65 | 5805 ± 95 | Wood fragments |
| 84 | 8230 ± 60 | 9205 ± 97 | Pollen-lignin-charcoal fraction |
| 140–150 (G) | 8750 ± 400 | 9841 ± 496 | Bulk organic matter |
| 160–200 (G) | 9005 ± 145 | 10093 ± 216 | Bulk organic matter |
| 450–460 (G) | 10980 ± 260 | 12933 ± 244 | Bulk organic matter |
| 640–665 (G) | 12500 ± 190 | 14765 ± 437 | Bulk organic matter |

phase was used to further separate the neutral fraction into apolar and polar fractions. The polar fraction contains the glycerol dialkyl glycerol tetraether (GDGT) lipids necessary for $TEX_{86}$ analysis. This polar fraction was filtered (0.45 μm filter), dried under $N_2$, then redissolved in 99:1 hexane:isopropanol for analysis. The apolar fraction containing *n*-alkanes was further separated into saturated and unsaturated hydrocarbons using Ag+ impregnated silica gel column chromatography as described in Castañeda et al. (2007).

### 2.2. GDGT analysis and $TEX_{86}$ as a temperature proxy

The $TEX_{86}$ paleotemperature proxy is based on the distribution of isoprenoid glycerol dialkyl glycerol tetraether (GDGT) lipids from aquatic Thaumarchaeota, which correlates with water temperature (Schouten et al., 2002; Kim et al., 2010) and has been used to reconstruct ancient SSTs back to 160 Ma (Jenkyns et al., 2012). GDGTs were analyzed by high performance liquid chromatography/atmospheric pressure chemical ionization mass spectrometry (HPLC/MS) as described in Schouten et al. (2007). GDGTs were analyzed using an Agilent 1100 series LC-MSD (Alltech Prevail Cyano column 150 × 2.1 mm; 3 μm) at 30 °C for separation. All runs were started with an isocratic elution for 5 min (flow rate of 0.2 ml/min), followed by a linear gradient to 1.8% isopropanol in 45 min. Detection was achieved using atmospheric pressure positive ion chemical ionization mass spectrometry (APCI-MS) of the eluent.

Analytical $TEX_{86}$ reproducibility for this study was determined using a series of replicates from a set of East African lakes run and integrated by the authors (n = 51 from Lakes Malawi, Turkana, Albert, and Victoria) (Berke et al., 2012a, 2012b). The relationship between mean annual lake surface temperatures (as a proxy for air temperatures) and $TEX_{86}$ values are calibrated using the equation for marine sediments, $TEX^H_{86}$ (Kim et al., 2010). The $TEX_{86}$ mean error of all duplicates is 0.007, with an average temperature of 0.3 °C using the $TEX^H_{86}$ calibration of Kim et al. (2010), plotted here for all Lake Albert $TEX_{86}$ values. This temperature calibration has an error estimation of ~2.5 °C based on global marine surface sediment samples (Kim et al., 2010). This calibration was chosen, instead of the global lake calibration of Powers et al. (2010) due to its ability to more closely reconstruct the range of Lake Albert water temperatures most likely seen in the Holocene based on known modern water temperatures at Lake Albert (Talling, 1963). The amplitude of temperature change through time is nearly identical using lacustrine or marine calibrations (Blaga et al., 2009; Kim et al., 2010; Powers et al., 2010; Tierney et al., 2010). While it is unclear why the global marine calibration provides the closest match to modern water temperatures at Lake Albert, a similar occurrence was documented in Lakes Turkana (Berke et al., 2012b) and Victoria (Berke et al., 2012a) and attributed to the possible lack of a permanent chemocline and anoxic deep water, which holds true for Lake Albert as well. Selection of one of the lacustrine calibrations (Blaga et al., 2009; Powers et al., 2010; Tierney et al., 2010) would shift the absolute temperature values slightly, but would not significantly alter the trends or amplitude of temperature variation discussed here.

Where there are large inputs of soil-derived isoprenoid tetraether compounds the $TEX_{86}$ paleotemperature proxy, which relies on the lipids derived from aquatic Thaumarchaeota, is not robust (Blaga et al., 2009; Powers et al., 2010; Sinninghe Damsté et al., 2012). Terrestrial influence is quantified using the BIT index, a ratio of predominantly soil-derived branched GDGTs to crenarchaeol lipids produced primarily by aquatic Thaumarchaeota, varying from predominantly aquatic (yielding a BIT of 0) to predominantly terrestrial (yielding a BIT of 1) (Hopmans et al., 2004). $TEX_{86}$ is not considered robust when BIT values exceed ~0.4 (Blaga et al., 2009; Powers et al., 2010); BIT values for this study were all less than 0.25.

### 2.3. $\delta^{13}C$ analysis and use as a proxy for vegetation change

The $\delta^{13}C$ values of leaf wax compounds (hereafter $\delta^{13}C_{wax}$) are here used to reconstruct changes in plant communities, with long-chain compounds (such as the *n*-alkanes used here) attributed primarily to epicuticular waxes from higher plants (Eglinton and Hamilton, 1967). The two $CO_2$ fixation pathways used by most terrestrial plants result in distinct isotope values (in both bulk and compound specific isotopes), allowing the use of $\delta^{13}C_{wax}$ to distinguish vegetation change (O'Leary, 1981). The metabolic pathways $C_3$ (found globally in shrubs, trees, and grasses) and $C_4$ (found in grasses and sedges) have differing enzymatic processes that govern how atmospheric $CO_2$ is utilized (O'Leary, 1981). The carbon concentrating mechanism employed by $C_4$ plants allows them to have an ecological advantage in warmer, drier, or low $pCO_2$ environments (Cerling et al., 1997; Ehleringer et al., 1997) due to their ability to curb possible desiccation by closing stomata and reducing transpiration and $CO_2$ loss. Thus, $C_4$ plants have a $^{13}C$-enriched signature compared to $C_3$ plants (Collister et al., 1994; Rieley et al., 1993). Additionally, there is a $\delta^{13}C$ signature associated with the carbon use efficiency in plants (Diefendorf et al., 2010), though if present, is likely to only to strengthen the direction of $C_3/C_4$ shifts with regard to changes in hydroclimate (described below).

The $\delta^{13}C$ of leaf wax *n*-alkanes were measured on an Agilent 6890N GC (60 m HP-1 column, 0.32-um diameter, 0.25 μm film thickness) interfaced to a Thermo Finnigan Delta$^{Plus}$ XP mass spectrometer. The GC temperature program began at 50 °C and increased at a rate of 50 °C/min to 180 °C followed by a rate of 3 °C/min to 320 °C. The final temperature of 320 °C was held for 6 min. The *n*-alkanes separated by the GC column were oxidized at 940 °C and converted to $CO_2$. A standard mixture of *n*-alkanes of known $\delta^{13}C$ values was analyzed multiple times daily ("Mix-A", $C_{16}$–$C_{30}$ provided by Dr. Arndt Schimmelmann, Indiana University), and based on these replicate measurements, typical precision of the $\delta^{13}C$ measurements were ±0.5‰ (1σ). Each sample was run in duplicate and co-injected with squalane to monitor reproducibility. Replicates of all $C_{29}$, $C_{31}$, and $C_{33}$ $\delta^{13}C$ values from Lake Albert sediments have a mean error of ±0.75‰. The $\delta^{13}C$ trends for $C_{29}$, $C_{31}$, and $C_{33}$ were generally similar and thus a weighted average ($C_{29}$–$C_{33}$) was used here. All $\delta^{13}C$ values are reported as per mil deviations from Vienna Pee Dee Belemnite (VPDB) standard using conventional delta notation.

### 2.4. δD analysis and use as proxy for precipitation amount

The most abundant leaf wax compounds, *n*-alkanoic acids (fatty acids), were used for δD analysis. Despite the high abundance of *n*-alkanoic acids relative to other leaf wax compounds, it was not sufficient to measure both δD and $\delta^{13}C$, thus *n*-alkanes were analyzed for $\delta^{13}C$ values in this study. The fatty acid fractions were methylated using 5% $BF_3$ in methanol (100 °C for 2 h) to produce fatty acid methyl esters (FAME). The FAME fraction was extracted using hexane and NaCl solution, using sodium sulfate columns to remove excess water

and cleaned with DCM followed by hexane elution through extracted Si gel. Palmitic acid of a known isotopic value was methylated to determine the isotopic composition of the attached methyl group. δD was also corrected for changes in ice volume and subsequent shifts in the δD of sea water (Konecky et al., 2011; Schrag et al., 1996; Tierney et al., 2011) and adjusted for shifts through time according to the LR04 benthic oxygen isotope stack (Lisiecki and Raymo, 2005).

The FAME δD values of leaf waxes (hereafter $\delta D_{wax}$) were determined using a MicroMass IsoPrime GC–IRMS with instrumental conditions outlined in Grice et al. (2008). $H_2$ gas of known isotopic value and high purity grade was injected as a reference gas standard. A mix of 6 FAMEs of known isotopic composition was run between samples to monitor instrument accuracy, with a mean error from duplicate analyses (reported here) of ±2.5‰. $C_{28}$ was the most abundant FAME homolog measured at Lake Albert and hereafter the $\delta D_{wax}$ refers specifically to the δD value of $C_{28}$ leaf wax. Sedimentary *n*-alkanoic acid homologs $C_{26}$–$C_{30}$ are thought to be supplied primarily from terrestrial higher plants (Volkman, 2006). The dominant FAME homolog found at Lake Albert matches that of other East African lake sites (Berke et al., 2012a; Costa et al., 2014; Konecky et al., 2011; Tierney et al., 2008, 2011) and provides additional confidence in the preservation of FAMEs at Lake Albert. All $\delta D_{wax}$ values are reported as per mil (‰) deviations from Vienna Standard Mean Ocean Water (VSMOW) in delta notation (Coplen, 2011).

The $\delta D_{wax}$ tracks source water δD with a biosynthetic fractionation offset (Sachse et al., 2012). The δD of tropical rainfall is inversely correlated with amount of precipitation, through Rayleigh distillation (Dansgaard, 1964; Rozanski et al., 1993), and thus times of increased aridity are linked to more D-enriched isotopes than wetter times. Influences on $\delta D_{wax}$ at Lake Albert beyond rainfall amount are considered secondary. For example, eastward migration of the CAB is limited by the Blue Mountains immediately to the west, leaving Lake Albert in an Atlantic moisture rain shadow (Camberlin, 2009). Thus, the rain source likely remained constant from the Indian Ocean. Further, while shifts in vegetation occurred, $\delta D_{wax}$ is unlikely to be solely an artifact of biosynthetic fractionation. Studies have shown that the difference in apparent fractionation of δD between $C_3$ trees and $C_4$ grasses may be small, or negligible (Sachse et al., 2012), without the presence of appreciable $C_3$ grasses. $C_3$ grasses have a significant difference in apparent fractionation (Smith and Freeman, 2006), but the majority of modern grasses <2000 m in East Africa (>90%) are $C_4$ (Livingstone and Clayton, 1980; Tieszen et al., 1979), an observation supported at Lake Albert (Beuning et al., 1997). Lastly, the role of humidity on $\delta D_{wax}$ is debated, but may exaggerate $\delta D_{wax}$ shifts. Hou et al. (2008) found a ~10‰ decrease in apparent fractionation for each 20% increase in humidity, so even with a possible humidity magnification of $\delta D_{wax}$, it is likely only a small fraction of the >40‰ shift seen in δD record from Lake Albert. We therefore attribute primary control on $\delta D_{wax}$ to changes in the Lake Albert regional precipitation amount.

## 3. Results & discussion

### 3.1. The climate of the Lake Albert region since the latest Pleistocene

A two-stage D-enrichment and $TEX_{86}$ decrease between 13.8 ka–11.5 ka shows that significant aridity accompanied cooling (Fig. 2). $\delta^{13}C_{wax}$ varies between −25 and −32‰ (Fig. 2). $C_4$ vegetation likely increased somewhat after 13.5 ka following the changes in temperature and moisture. The peak in $C_4$ plants at 12.3 ka agrees with dry conditions interpreted from D-enrichment. The $\delta^{13}C_{wax}$ record indicates a continuous protracted reduction in $C_4$ plants after the YD that continued until 10.1 ka.

Comparison of $\delta^{13}C_{wax}$ with a fossil pollen record from Lake Albert (Beuning et al., 1997) suggests these proxies are recording similar though not identical aspects of vegetation. The onset and termination of cooling between 13.8 and 11.5 ka is synchronous with an extended

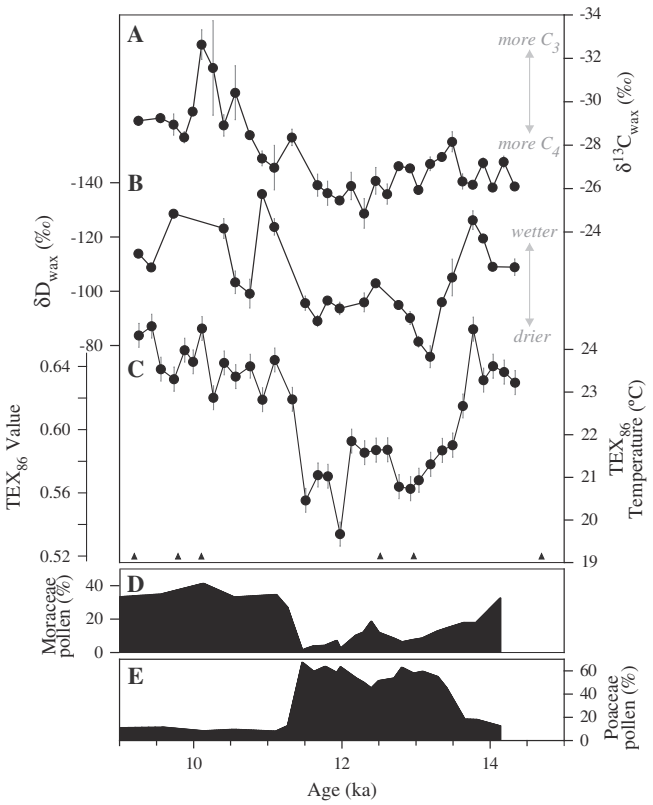


**Fig. 2.** Lake Albert records. (A) $\delta^{13}C_{wax}$ (B) $\delta D_{wax}$ (C) $TEX_{86}$ paleotemperatures (°C). Error bars are standard deviation of replicate analyses for each sample (isotopes) or group of replicates ($TEX_{86}$). Pollen analyses of Beuning et al. (1997) for (D) Poaceae (grasses) and (E) Moraceae (trees/shrubs) from the same core. $^{14}C$ dates represented by axis triangles.

period of aridity, as marked by a pronounced increase in grasses and reduction of semi-deciduous forest taxa (Fig. 2). This period of pollen-inferred aridity is interrupted by slightly wetter conditions ~12.8–12.3 ka, shown by a decrease in open grassland and slight recovery of Moraceae forest taxa. This pollen shift is correlative with moderate transient warming (~12.6–12.1 ka) and a modest shift to D-depleted values within the otherwise cold, arid interval.

A $^{13}C$-enrichment of 3‰ occurs during a pronounced grassland increase at the beginning of the Lake Albert record (~13.8–12.5 ka) but the protracted $^{13}C$-depletion in the early Holocene is not identical in timing with grassland disappearance (Fig. 2). Although $C_3$ grasses are not expected to contribute significantly to this record, one possible explanation is that while $C_4$ grassland dominated, the remainder could be supplied by $C_3$ grasses, contributing more Poaceae pollen and "muted" $^{13}C$-enrichment. Alternatively, $CO_2$ by this time was higher (Monnin et al., 2001) and temperatures were cooler, potentially balancing the tendency for relative aridity to allow $C_4$ vegetation to flourish (Sinninghe Damsté et al., 2011). Lastly, differences in production or residence time before deposition may factor into temporal differences between pollen and *n*-alkane records.

### 3.2. Controls on $\delta D_{wax}$ at Lake Albert

We observe a similar trend in the pollen and $\delta D_{wax}$ records in Lake Albert (Fig. 2); the shifts in $\delta D_{wax}$ do not align precisely with shifts in the dominant pollen, suggesting changing vegetation does not significantly alter $\delta D_{wax}$ values. Further, apparent fractionations for $C_{28}$ fatty acids were described for a $C_4$ grass (127 ± 6‰) and $C_3$ tree (114 ± 8‰) (Hou et al., 2008). The apparent fractionation of $\delta D_{wax}$ appears to be relatively constant along field transects with variable $C_3/C_4$ vegetation, correlating linearly with rainfall in Europe (Hou et al., 2008; Sachse et al., 2004) and in the southwestern

USA (Feakins and Sessions, 2010; Hou et al., 2008). Additionally, a transect of surface sediments from lakes across Cameroon (west Central Africa) found that $\delta D_{wax}$ of long chain *n*-alkanes served well as a proxy of regional source water, and that changes between $C_3$ and $C_4$ photosynthetic pathway could not explain variations seen in $\delta D_{wax}$ (Garcin et al., 2012). This consistency may imply that a regional integration of isotopic fractionation is preserved in sediments and differences in vegetation play a smaller role at broad scales. The $\delta^{13}C_{wax}$ record from Lake Albert shows significant changes from a Moraceae-dominated ($C_3$ trees/shrubs) landscape to a Poaceae-dominated ($C_4$ grasses) landscape (Fig. 2). Yet a shift to a $C_3$-tree dominated environment in the early Holocene at Lake Albert does not appear to reduce apparent fractionation (which would be demonstrated through a shift to less D-depleted values) and suggests $\delta D_{wax}$ is not controlled by vegetation type, supporting our assumption of the independence of $\delta D_{wax}$ from major vegetation changes. Beyond vegetation controls on $\delta D_{wax}$, the influence of temperature on $\delta D_{wax}$ values of precipitation is also considered negligible in the tropics (Araguás-Araguás et al., 2000; Dansgaard, 1964; Rozanski et al., 1993). Consequently the variability in $\delta D_{wax}$ seen at Lake Albert is here ascribed to changes in the regional hydroclimate, with little influence from changes in terrestrial vegetation.

### 3.3. A regional view of climate change across the last deglacial in East Africa

The emerging regional pattern from African continental paleotemperature records at low elevations (<1000 m above sea level) shows a departure from a progressive deglacial warming, evident in a 2 °C cooling for Lake Malawi (Powers et al., 2005), ~1 °C for Lake Tanganyika (Tierney et al., 2008), and a pause in warming for Lake Victoria (Berke et al., 2012a) and the Congo Basin (Weijers et al., 2007) and a gradual increase in temperature at Lake Challa (Sinninghe Damsté et al., 2012) spanning ~14 to 11.5 ka (Fig. 3). The magnitude of temperature change seen at Lake Albert (ca. 3 °C) is surprisingly large in comparison to the aforementioned African records or modeling

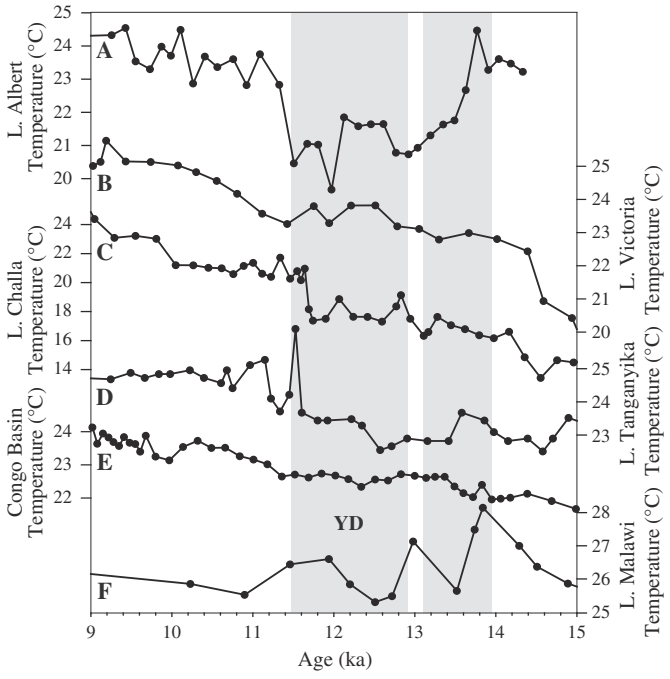


**Fig. 3.** Select continental molecular temperature records from Africa (in °C), Lake Albert (A), Lake Victoria $TEX_{86}$ (Berke et al., 2012a) (B), Lake Challa MBT/CBT (Sinninghe Damsté et al., 2012) (C), Lake Tanganyika $TEX_{86}$ (Tierney et al., 2008) (D), Congo Basin MBT/CBT (Weijers et al., 2007), (E), Lake Malawi $TEX_{86}$ (Powers et al., 2005) (F). Gray bars indicate Younger Dryas (YD) and the early deglacial hydroclimate transition described in the text.

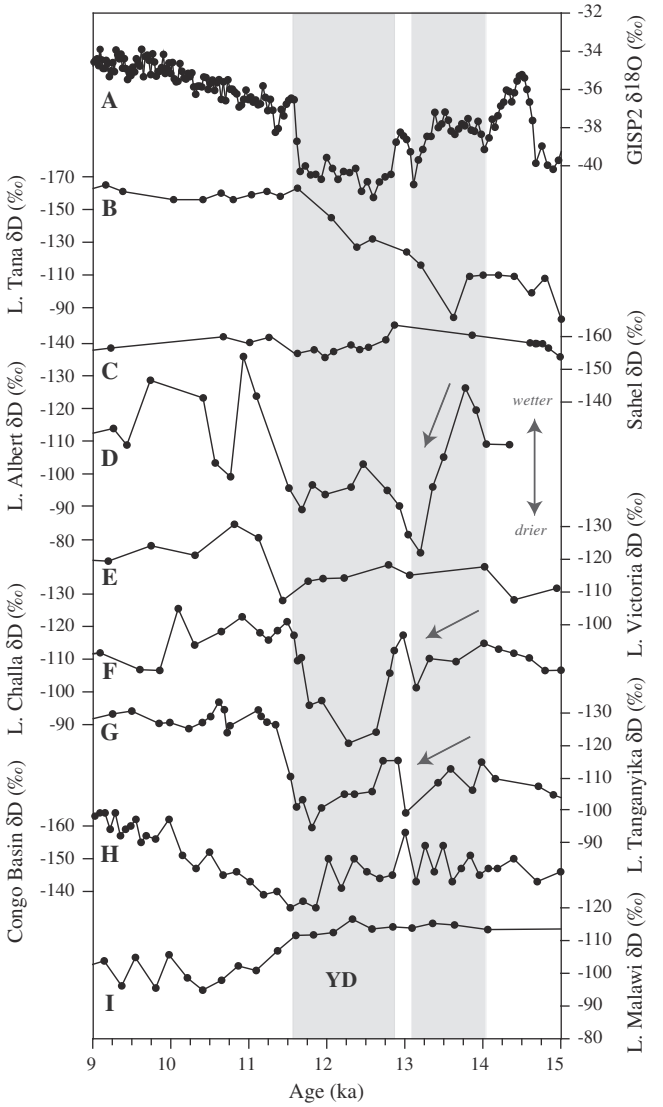


**Fig. 4.** Greenland ice core $\delta^{18}O$ (Grootes et al., 1993) (A) compared to select continental molecular δD records from Africa, Lake Tana $C_{28}$ *n*-alkanoic acid (Costa et al., 2014) (B), Sahel $C_{31}$ *n*-alkane (Niedermeyer et al., 2010) (C), Lake Albert $C_{28}$ *n*-alkanoic acid (D), Lake Victoria $C_{28}$ *n*-alkanoic acid (Berke et al., 2012a) (E), Lake Challa $C_{28}$ *n*-alkanoic acid (Tierney et al., 2011) (F), Lake Tanganyika $C_{28}$ *n*-alkanoic acid (Tierney et al., 2008) (G), Congo Basin $C_{29}$ *n*-alkane (Schefuß et al., 2005) (H), Lake Malawi $C_{28}$ *n*-alkanoic acid (Konecky et al., 2011) (I). Gray bars indicate Younger Dryas (YD) and the early deglacial hydroclimate transition aligning with the OD described in the text. Arrows highlight the pattern of D-enrichment between 14 and 13 ka.

results of the tropics (Liu et al., 2009). Lakes Tanganyika, Malawi, and Albert begin cooling ~13.8–13.6 ka and while Lakes Malawi and Tanganyika reached temperature minima at ~13.4 ka, Lake Albert continued to cool until ~12.9 ka.

Hydroclimate proxies show a shift to arid conditions around the YD in Africa, even in regions with little to no cooling (Fig. 4). Lake level estimates in and around equatorial Africa show a significant decrease during the YD (deMenocal et al., 2000; Gasse, 2000; Gasse et al., 2008; Olago et al., 2000). YD aridity extended north to parts of the Sahara (Gasse et al., 1990) and the Sahel (Gasse, 2000; Street-Perrott and Perrott, 1990), more recently confirmed by minor leaf wax D-enrichment and supported by $\delta^{13}C$ (Niedermeyer et al., 2010). Significant aridity interpreted from a leaf wax δD reconstruction and increased $C_4$ vegetation at the YD is observed without associated cooling in the Congo Basin (Schefuß et al., 2005). The Lake Challa δD record shows a shift comparable to Lake Albert $\delta D_{wax}$, with

a 30‰ D-enrichment during the YD as well as D-enrichment between 14–13 ka of ~15‰ (Tierney et al., 2011). An interval of minor, yet variable D-enrichment begins at ~14 ka at Lake Tanganyika, preceding the YD and roughly coincident with initiation of the cool, dry interval in Lake Albert. Lake Tanganyika also shows a 23‰ D-depletion at the end of the YD, signaling that while there may be little to no δD shift into this interval, an increase in moisture can be seen at its termination (Tierney et al., 2008). While the δD record at Lake Malawi has been attributed to changes in atmospheric circulation (Konecky et al., 2011), a record of $\delta^{13}C_{wax}$ used as a secondary proxy for aridity (Castañeda et al., 2007), showed a decrease in humid conditions at Lake Malawi during the YD. A new δD record from Lake Tana, Ethiopia shows the only significant D-enrichment of ~70‰ across the deglacial interval (Costa et al., 2014).

### 3.4. Forcing mechanisms of Lake Albert climate

We observe general aridity with varying intensities and durations, supported by molecular and other sedimentological proxies (Gasse, 2000), particularly with respect to the recovery to less arid conditions during the deglaciation from the latest Pleistocene to early Holocene in East Africa. The Late Pleistocene brief cooling and drying that preceded the YD ~14 ka at Lakes Albert, Challa, and Tanganyika (Figs. 3, 4) is mechanistically perplexing. The spatial and temporal heterogeneity in tropical Africa at this time interval implies a complex climate pattern across the continent, perhaps due to variations in moisture source or regional internal climate drivers. Western African regions do not experience increased aridity at 14 ka (Schefuß et al., 2005) while other records do not have sufficient resolution to fully address changes during the interval from 14–13 ka, such as at Lake Victoria (Berke et al., 2012a) or the Sahel (Niedermeyer et al., 2010). However, available reconstructions indicate a network of climate regimes across the region that mimic modern African climatology, where complex topography and multiple drivers control regional cloud cover, temperature, and rainfall delivery (Camberlin, 2009).

We note that cooling and drying occurred during the deglaciation in East Africa, particularly at Lake Albert, but began earlier than the YD, at a time of significant global change. Lake Albert cooling began ~13.8 ka (Fig. 2) and is coincident within age model error of cooling in Greenland (Grootes et al., 1993) and the OD, and follows the ACR. The ACR may have occurred from northward migration of the Subtropical Front (Putnam et al., 2010), altering the Agulhas current and reducing leakage of Indian Ocean water to the Atlantic Ocean around Africa (Beal et al., 2011). Reduced input from the Indian Ocean has been shown in model (Weijer et al., 2002) and proxy studies (Chiessi et al., 2008) to have weakened the AMOC during the last deglaciation stadials, reducing cross basin exchange (Bard and Rickaby, 2009). Modeling has linked freshwater input to the Atlantic to an arid western Indian Ocean (Zhang and Delworth, 2005). Likewise, reconstruction of the AMOC using $^{231}Pa/^{230}Th$ shows an inflection in the slope of reconstructed AMOC strength at ~14 ka suggesting a minor reduction in circulation strength (McManus et al., 2004). This is supported by $\delta^{13}C$ values of benthic foraminifera, a proxy of deep water ventilation and AMOC strength (Vidal et al., 1997). Recently, Ritz et al. (2013) used temperature proxy reconstructions and model simulation hindcasting to reconstruct AMOC strength. Their results support the $^{231}Pa/^{230}Th$ reconstruction of McManus et al. (2004), and seem to indicate that while AMOC anomalies were high, there was a minor reduction in the AMOC rate at ~14 ka, the first decline of any kind since the LGM. This possible AMOC suppression, while not as rapid or significant as at the YD, may have been sufficient to cause an Indian Oceanic disturbance, which in turn is thought to trigger cool, arid conditions in regions of East Africa.

This stadial was a time of variable, but overall decreasing temperatures in the northern high latitudes as indicated by $\delta^{18}O$ in the GISP2 ice core (Alley and Clark, 1999; Grootes et al., 1993). The North Atlantic experienced cooling of surface water temperatures (Bard et al., 2000; Waelbroeck et al., 1998). Speleothem records demonstrate teleconnections between the climates of Greenland and the Indian Ocean, with drier (wetter) conditions associated with stadials (interstadials) in the North Atlantic (Burns et al., 2003; Shakun et al., 2007). Further, a $\delta^{18}O$ speleothem record from Socotra Island, Yemen shows an increase in dry conditions in the Indian Ocean with timing roughly equivalent to cooler Greenland temperatures while also varying in concert with a sedimentary $\delta^{15}N$ record from the Indian Ocean, a proxy of denitrification (Ivanochko et al., 2005). Reduced denitrification has been attributed to a reduction of wind-driven upwelling productivity from a weaker Indian Monsoon during Greenland stadials (Altabet et al., 2002). These paleoclimate records all support a change in the Indian Ocean monsoon ~14 ka. Verschuren et al. (2009) proposed from their Lake Challa record that during stadial events, northern polar ice influence and a reduction of Indian Ocean SSTs overshadowed regional insolation controls.

Within dating uncertainty, the described cooling in Greenland around the OD aligns well with the spatially complex pattern of cooling and drying in East Africa beginning in the latest Pleistocene preceding the YD. Here, we link these conditions to a weakened Indian monsoon that may have been affected by changes in the AMOC and Agulhas leakage into the Atlantic (Stenni et al., 2001). The pressure gradient that is established between hemispheres can force tropical surface winds and reduce the monsoonal system in the region as the ITCZ is shifted southward (Chiang and Friedman, 2012).

Among the paleoclimate records now available for tropical Africa that cover the last deglaciation, the Lake Albert basin appears to have responded most dramatically to the OD and YD stadials. Temperatures began cooling at 13.8 ka and continued cooling by more than 3 °C by 12.9 ka and more by the end of the YD. None of the other African records display such cooling: the Malawi basin cooled ~2 °C, Tanganyika cooled only 1 °C, and no other African sites display any measurable cooling. The Albert basin also experienced the greatest reduction in rainfall of all of the African sites investigated to date, as indicated by the 40‰ D-enrichment, which surpasses even that observed at Lake Challa (~30‰) (Tierney et al., 2011) or Lake Tanganyika (~20‰) (Tierney et al., 2008).

It is unclear why the climate response of the Albert basin was more extreme than that of other African sites that have been analyzed thus far for their deglacial history. Lake Albert is situated farther inland than any of the other sites, so perhaps its temperature is not ameliorated as much by maritime influence and its aridity is also more severe due to its more distal location from the Indian Ocean.

The coincident shift to more arid conditions during the YD in both Lake Challa and Lake Albert runs counter to the decadal–centennial pattern of rainfall variability in East Africa reported by Tierney et al. (2013). This pattern exhibits an anti-phased relationship between rainfall in the Rift Valley where Lake Albert and Lake Tanganyika lie, and more coastal East Africa, where Lake Challa is found. This pattern of rainfall is attributed to the zonal gradient of SSTs in the Indian Ocean, which is not necessarily tied to the effects of North Atlantic stadial conditions that are considered to have caused the YD.

Recently, studies from around East Africa have documented past CAB movements and an influence of Atlantic-derived moisture that appear to explain past hydrological conditions (Costa et al., 2014; Junginger and Trauth, 2013). Similarly, moisture at Central and West African sites is often attributed to an Atlantic Ocean source (Niedermeyer et al., 2010; Schefuß et al., 2005). We suggest that Lake Albert was primarily isolated from Atlantic-sourced moisture due to regional orography, as has been suggested for much of easternmost Africa (Tierney et al., 2011). $\delta D_{wax}$ records from predominantly Indian Ocean-influenced regions including Lakes Albert, Challa (Tierney et al., 2011), and Tanganyika (Tierney et al., 2008) indicate an OD drying interval and on average more D-enriched leaf wax compounds. Those that have been suggested to have more Atlantic Ocean moisture influence including the Sahel (Niedermeyer et al., 2010), Congo Basin

(Schefuß et al., 2005), and Lake Tana (Costa et al., 2014) do not appear to show an initial stage of drying at the OD and indicate more similar δD values to each other (generally more D-depleted during OD and YD) than those records to the east seemingly less affected by Atlantic Ocean moisture.

As meso-scale models of climate dynamics in East Africa are further developed, taking into account the effects of regional topography and lake-feedback effects, the paleoclimate records of Lake Albert and other sites on the African continent will provide excellent opportunities for testing future model validity.

## 4. Conclusions

New organic geochemical reconstructions from Lake Albert allow us to investigate changes in East African climate from the Late Pleistocene to early Holocene. We observe an unusually strong response to the OD and YD, with multi-stage cooling in a record of $TEX_{86}$ paleotemperatures between 13.8 and 11.5 ka. Changes in hydroclimate, as evidenced from a D-enrichment from leaf wax FAMEs, support the interpretation that this region also experienced unusually pronounced drying during this interval. Regional vegetation records, including previously analyzed pollen and newly added leaf wax *n*-alkane $\delta^{13}C$, show that vegetation responded to these shifts, with increasing $C_4$ vegetation (Poaceae pollen) during cool, arid intervals and increasing $C_3$ vegetation (Moraceae pollen) during warmer and less arid intervals.

Multi-stage cool, dry conditions at Lake Albert began prior to the YD, at a globally significant time that coincides with the Older Dryas. This coincides with the beginning of stepwise cooling in Greenland, a decrease in the rate of the AMOC for the first time since the LGM, and a reduction of the Indian Ocean monsoon. We interpret the observed changes at Lake Albert during this interval as the manifestation of changes incurred to the monsoon and ultimately monsoonal moisture delivery to Lake Albert. While there are multiple paleorecords that indicate a shift, particularly in hydroclimate, ~14 ka, regional complexity in climate reconstructions between African sites emphasizes the heterogeneous patterns of climate across the continent and the importance of regional drivers. The complex pattern of East African climate response to the influence of shifting conditions in the North Atlantic Ocean during the last deglaciation underscores the need for the development of more refined models of climate dynamics in East Africa, not only to better comprehend the past but, more importantly, to be able to more accurately predict future trends in this heavily populated region.

## Acknowledgments

We thank Ellen Hopmans, Jort Ossebaar, Sarah Grosshuesch, Koushik Dutta, Stephen Clayton, and Geoff Chidlow. Research was funded by grant NA-060-AR4310113 (NOAA and the EU Seventh Framework Programme (FP7/2007e2013)/ERC grant agreement no. [226600]. Support also acknowledged from EAOG Grant (to M.B.). Core collection, shipment and curation were supported by NSF grants GB8328X, GB22858, GB 33310 and BMS-75-034-54. Commissioner C. E. Tamale-Ssali of the Uganda Geological Survey and Mines Department authorized the field work. John Okedi, Director of EAFFRO, and S.N. Semakula, P.J. Omedo and Peter Karakaba of the Fisheries Department generously shared their space, equipment, and wisdom. The seamanship, stamina and strength of William Karamanyire and Francisco Rwaswire were essential to success of the field work.

## References

Alley, R.B., Clark, P.U., 1999. The deglaciation of the Northern Hemisphere: a global perspective. AREPS 27, 149–182.

Altabet, M.A., Higginson, M.J., Murray, D.W., 2002. The effect of millennial-scale changes in Arabian Sea denitrification on atmospheric $CO_2$. Nature 415, 159–162.

Araguás-Araguás, L., Froehlich, K., Rozanski, K., 2000. Deuterium and oxygen-18 isotope composition of precipitation and atmospheric moisture. HyPr 14, 1341–1355.

Bard, E., Rickaby, R.E.M., 2009. Migration of the subtropical front as a modulator of glacial climate. Nature 460, 380–383.

Bard, E., Rostek, F., Turon, J.-L., Gendreau, S., 2000. Hydrological impact of Heinrich events in the subtropical northeast Atlantic. Science 289, 1321–1324.

Beal, L.M., De Ruijter, W.P.M., Biastoch, A., Zahn, R., 2011. On the role of the Agulhas system in ocean circulation and climate. Nature 472, 429–436.

Berke, M.A., Johnson, T.C., Werne, J.P., Grice, K., Schouten, S., Sinninghe Damsté, J.S., 2012a. Molecular records of climate variability and vegetation response since the Late Pleistocene in the Lake Victoria basin, East Africa. Quat. Sci. Rev. 55, 59–74.

Berke, M.A., Johnson, T.C., Werne, J.P., Schouten, S., Sinninghe Damsté, J.S., 2012b. A mid-Holocene thermal maximum at the end of the African Humid Period. Earth Planet. Sci. Lett. 95–104.

Beuning, K.R., Talbot, M.R., Kelts, K., 1997. A revised 30,000-year paleoclimatic and paleohydrologic history of Lake Albert, East Africa. Palaeogeogr. Palaeoclimatol. Palaeoecol. 136, 259–279.

Blaga, C., Reichart, G.-J., Heiri, O., Sinninghe Damsté, J., 2009. Tetraether membrane lipid distributions in water-column particulate matter and sediments: a study of 47 European lakes along a north–south transect. J. Paleolimnol. 41, 523–540.

Broecker, W.S., 1998. Paleocean circulation during the Last Deglaciation: a bipolar seesaw? Paleoceanography 13, 119.

Burns, S.J., Fleitmann, D., Matter, A., Kramers, J., Al-Subbary, A.A., 2003. Indian Ocean climate and an absolute chronology over Dansgaard/Oeschger Events 9 to 13. Science 301, 1365–1367.

Camberlin, P., 2009. Nile Basin climates. In: Dumont, H.J. (Ed.), The Nile: Origin, Environments, Limnology and Human Use. Springer, pp. 307–333.

Castañeda, I.S., Werne, J., Johnson, T.C., 2007. Wet and arid phases in the southeast African tropics since the Last Glacial Maximum. Geology 35, 823–826.

Cerling, T.E., Harris, J.M., MacFadden, B.J., Leakey, M.G., Quade, J., Eisenmann, V., Ehleringer, J.R., 1997. Global vegetation change through the Miocene/Pliocene boundary. Nature 389, 153–158.

Chiang, J.C.H., Friedman, A.R., 2012. Extratropical cooling, interhemispheric thermal gradients, and tropical climate change. AREPS 40, 383–412.

Chiessi, C.M., Mulitza, S., Paul, A., Pätzold, J., Groeneveld, J., Wefer, G., 2008. South Atlantic interocean exchange as the trigger for the Bølling warm event. Geology 36, 919–922.

Collister, J.W., Rieley, G., Stern, B., Eglinton, G., Fry, B., 1994. Compound-specific $\delta^{13}C$ analyses of leaf lipids from plants with differing carbon dioxide metabolisms. Org. Geochem. 21, 619–627.

Coplen, T.B., 2011. Guidelines and recommended terms for expression of stable-isotope-ratio and gas-ratio measurement results. Rapid Commun. Mass Spectrom. 25, 2538–2560.

Costa, K., Russell, J., Konecky, B., Lamb, H., 2014. Isotopic reconstruction of the African Humid Period and Congo Air Boundary migration at Lake Tana, Ethiopia. Quat. Sci. Rev. 83, 58–67.

Dansgaard, W., 1964. Stable isotopes in precipitation. Tellus 16, 436–468.

deMenocal, P., Ortiz, J., Guilderson, T., Adkins, J., Sarnthein, M., Baker, L., Yarusinsky, M., 2000. Abrupt onset and termination of the African Humid Period: rapid climate responses to gradual insolation forcing. Quat. Sci. Rev. 19, 347–361.

Diefendorf, A.F., Mueller, K.E., Wing, S.L., Koch, P.L., Freeman, K.H., 2010. Global patterns in leaf 13C discrimination and implications for studies of past and future climate. Proc. Natl. Acad. Sci. 107, 5738–5743.

Eglinton, G., Hamilton, R.J., 1967. Leaf epicuticular waxes. Science 156, 1322–1335.

Ehleringer, J.R., Cerling, T.E., Helliker, B.R., 1997. $C_4$ photosynthesis, atmospheric $CO_2$, and climate. Oecologia 112, 285–299.

Feakins, S.J., Sessions, A.L., 2010. Controls on the D/H ratios of plant leaf waxes in an arid ecosystem. Geochim. Cosmochim. Acta 74, 2128–2141.

Garcin, Y., Schwab, V.F., Gleixner, G., Kahmen, A., Todou, G., Séné, O., Onana, J.-M., Achoundong, G., Sachse, D., 2012. Hydrogen isotope ratios of lacustrine sedimentary n-alkanes as proxies of tropical African hydrology: insights from a calibration transect across Cameroon. Geochim. Cosmochim. Acta 79, 106–126.

Gasse, F., 2000. Hydrological changes in the African tropics since the Last Glacial Maximum. Quat. Sci. Rev. 19, 189–211.

Gasse, F., TeHhet, R., Durand, A., Gibert, E., Fontes, J.C., 1990. The arid-humid transition in the Sahara and the Sahel during the last deglaciation. Nature 346, 141–156.

Gasse, F., Chalié, F., Vincens, A., Williams, M.A.J., Williamson, D., 2008. Climatic patterns in equatorial and southern Africa from 30,000 to 10,000 years ago reconstructed from terrestrial and near-shore proxy data. Quat. Sci. Rev. 27, 2316.

Grice, K., Yu, H., Zhou, Y.P., Stuart-Williams, H., Farquhar, G.D., 2008. Biosynthetic and environmental effects on the stable carbon isotopic compositions of anteiso-(3-methyl) and iso-(2-methyl) alkanes in tobacco leaves. Phytochemistry 69, 2807–2814.

Grootes, P.M., Stuiver, M., White, J.W.C., Johnsen, S., Jouzel, J., 1993. Comparison of oxygen isotope records from the GISP2 and GRIP Greenland ice cores. Nature 366, 552–554.

Harvey, T., 1976. The Paleolimnology of Lake Mobutu Sese Seko, Uganda Zaire: The Last 28,000 Years. , Duke University.

Hopmans, E.C., Weijers, J.W.H., Schefuß, E., Herfort, L., Sinninghe Damsté, J.S., 2004. A novel proxy for terrestrial organic matter in sediments based on branched and isoprenoid tetraether lipids. Earth Planet. Sci. Lett. 224, 107–116.

Hou, J., D'Andrea, W.J., Huang, Y., 2008. Can sedimentary leaf waxes record D/H ratios of continental precipitation? Field, model, and experimental assessments. Geochim. Cosmochim. Acta 72, 3503–3517.

Ivanochko, T.S., Ganeshram, R.S., Brummer, G.-J.A., Ganssen, G., Jung, S.J.A., Moreton, S.G., Kroon, D., 2005. Variations in tropical convection as an amplifier of global climate change at the millennial scale. Earth Planet. Sci. Lett. 235, 302–314.

Jenkyns, H.C., Schouten-Huibers, L., Schouten, S., Sinninghe Damsté, J.S., 2012. Warm Middle Jurassic–Early Cretaceous high-latitude sea-surface temperatures from the Southern Ocean. Clim. Past 8, 215–226.

Jouzel, J., Vaikmae, R., Petit, J.-R., Martin, M., Duclos, Y., Stievenard, M., Lorius, C., Toots, M., Melie'res, M.-A., Burckle, L.H., Barkov, N.I., Kotlyakov, V.M., 1995. The two-step shape and timing of the last deglaciation in Antarctica. ClDy 11, 151–161.

Junginger, A., Trauth, M.H., 2013. Hydrological constraints of paleo-Lake Suguta in the Northern Kenya Rift during the African Humid Period (15–5 ka BP). Glob. Planet. Change 111, 174–188.

Kim, J.-H., van der Meer, J., Schouten, S., Helmke, P., Willmott, V., Sangiorgi, F., Koç, N., Hopmans, E.C., Sinninghe Damsté, J.S., 2010. New indices and calibrations derived from the distribution of crenarchaeal isoprenoid tetraether lipids: implications for past sea surface temperature reconstructions. Geochim. Cosmochim. Acta 74, 4639–4654.

Konecky, B.L., Russell, J.M., Johnson, T.C., Brown, E.T., Berke, M.A., Werne, J.P., Huang, Y., 2011. Atmospheric circulation patterns during late Pleistocene climate changes at Lake Malawi, Africa. Earth Planet. Sci. Lett. 312, 318–326.

Lisiecki, L.E., Raymo, M.E., 2005. A Pliocene–Pleistocene stack of 57 globally distributed benthic $\delta^{18}O$ records. Paleoceanography 20, PA1003.

Liu, Z., Otto-Bliesner, B.L., He, F., Brady, E.C., Tomas, R., Clark, P.U., Carlson, A.E., Lynch-Stieglitz, J., Curry, W., Brook, E., Erickson, D., Jacob, R., Kutzbach, J., Cheng, J., 2009. Transient simulation of last deglaciation with a new mechanism for Bølling-Allerød warming. Science 325, 310–314.

Livingstone, D.A., Clayton, W.D., 1980. An altitudinal cline in tropical African grass floras and its paleoecological significance. Quat. Res. 13, 392–402.

McManus, J.F., Francois, R., Gherardi, J.M., Keigwin, L.D., Brown-Leger, S., 2004. Collapse and rapid resumption of Atlantic meridional circulation linked to deglacial climate changes. Nature 428, 834–837.

Monnin, E., Indermühle, A., Dällenbach, A., Flückiger, J., Stauffer, B., Stocker, T.F., Raynaud, D., Barnola, J.-M., 2001. Atmospheric $CO_2$ concentrations over the Last Glacial Termination. Science 291, 112–114.

Nicholson, S.E., 1996. A review of climate dynamics and climate variability in eastern Africa. In: Johnson, T.C., Odada, E.O. (Eds.), The Limnology, Climatology, and Paleoclimatology of the East African Rift Lakes. Gordon and Breach, Amsterdam, pp. 25–56.

Niedermeyer, E.M., Schefuß, E., Sessions, A.L., Mulitza, S., Mollenhauer, G., Schulz, M., Wefer, G., 2010. Orbital- and millennial-scale changes in the hydrologic cycle and vegetation in the western African Sahel: insights from individual plant wax δD and $\delta^{13}C$. Quat. Sci. Rev. 29, 2996–3005.

Olago, D.O., Street-Perrott, F.A., Perrott, R.A., Ivanovich, M., Harkness, D.D., 2000. Long-term temporal characteristics of paleomonsoon dynamics in equatorial Africa. Glob. Planet. Change 26, 159–171.

O'Leary, M.H., 1981. Carbon isotope fractionation in plants. Phytochemistry 20, 553–567.

Powers, L.A., Johnson, T.C., Werne, J.P., Castañeda, I., Hopmans, E.C., Sinninghe Damsté, J.S., Schouten, S., 2005. Large temperature variability in the southern African tropics since the Last Glacial Maximum. Geophys. Res. Lett. 32, L08706. http://dx.doi.org/10.01029/02004GL022014.

Powers, L.A., Werne, J.P., Van der woude, A.J., Sinninghe Damsté, J.S., Hopmans, E.C., Schouten, S., 2010. Applicability and calibration of the $TEX_{86}$ paleothermometer in lakes. Org. Geochem. 41, 404–413.

Putnam, A.E., Denton, G.H., Schaefer, J.M., Barrell, D.J.A., Andersen, B.G., Finkel, R.C., Schwartz, R., Doughty, A.M., Kaplan, M.R., Schluchter, C., 2010. Glacier advance in southern middle-latitudes during the Antarctic Cold Reversal. Nat. Geosci. 3, 700–704.

Rieley, G., Collister, J.W., Stern, B., Eglinton, G., 1993. Gas chromatography/isotope ratio mass spectrometry of leaf wax *n*-alkanes from plants of differing carbon dioxide metabolisms. Rapid Commun. Mass Spectrom. 7, 488–491.

Ritz, S.P., Stocker, T.F., Grimalt, J.O., Menviel, L., Timmermann, A., 2013. Estimated strength of the Atlantic overturning circulation during the last deglaciation. Nat. Geosci. 6, 208–212.

Rozanski, K., Araguas-Araguas, L., Gonfiantini, R., 1993. Isotopic patterns in modem global precipitation. In: Swart, P.K., Lohmann, K.C., McKenzie, J.A., Savin, S. (Eds.), Climate Change in Continental Isotopic Records AGU Monograph, pp. 1–36.

Sachse, D., Radke, J., Gleixner, G., 2004. Hydrogen isotope ratios of recent lacustrine sedimentary *n*-alkanes record modern climate variability. Geochim. Cosmochim. Acta 68, 4877–4889.

Sachse, D., Billault, I., Bowen, G.J., Chikaraishi, Y., Dawson, T.E., Feakins, S.J., Freeman, K.H., Magill, C.R., McInerney, F.A., van der Meer, M.T.J., Polissar, P., Robins, R.J., Sachs, J.P., Schmidt, H.-L., Sessions, A.L., White, J.W.C., West, J.B., Kahmen, A., 2012. Molecular paleohydrology: Interpreting the hydrogen-isotopic composition of lipid biomarkers from photosynthesizing organisms. AREPS 40, 221–249.

Schefuß, E., Schouten, S., Schneider, R.R., 2005. Central African hydrologic changes during the past 20,000 years. Nature 437, 1003–1006.

Schouten, S., Hopmans, E.C., Schefuß, E., Sinninghe Damsté, J.S., 2002. Distributional variations in marine crenarchaeotal membrane lipids: a new tool for reconstructing ancient sea water temperatures? Earth Planet. Sci. Lett. 204, 265–274.

Schouten, S., Huguet, C., Hopmans, E.C., Kienhuis, M.V.M., Sinninghe Damsté, J.S., 2007. Analytical methodology for $TEX_{86}$ paleothermometry by high-performance liquid chromatography/atmospheric pressure chemical ionization-mass spectrometry. Anal. Chem. 79, 2940–2944.

Schrag, D.P., Hampt, G., Murray, D.W., 1996. Pore fluid constraints on the temperature and oxygen isotopic composition of the glacial ocean. Science 272, 1930–1932.

Shakun, J.D., Carlson, A.E., 2010. A global perspective on Last Glacial Maximum to Holocene climate change. Quat. Sci. Rev. 29, 1801.

Shakun, J.D., Burns, S.J., Fleitmann, D., Kramers, J., Matter, A., Al-Subary, A., 2007. A high-resolution, absolute-dated deglacial speleothem record of Indian Ocean climate from Socotra Island, Yemen. Earth Planet. Sci. Lett. 259, 442–456.

Sinninghe Damsté, J.S., Verschuren, D., Ossebaar, J., Blokker, J., van Houten, R., van der Meer, M.T.J., Plessen, B., Schouten, S., 2011. A 25,000-year record of climate-induced changes in lowland vegetation of eastern equatorial Africa revealed by the stable carbon-isotopic composition of fossil plant leaf waxes. Earth Planet. Sci. Lett. 302, 236–246.

Sinninghe Damsté, J.S., Ossebaar, J., Schouten, S., Verschuren, D., 2012. Distribution of tetraether lipids in the 25-ka sedimentary record of Lake Challa: extracting reliable TEX86 and MBT/CBT palaeotemperatures from an equatorial African lake. Quat. Sci. Rev. 50, 43–54.

Smith, F.A., Freeman, K.H., 2006. Influence of physiology and climate on δD of leaf wax *n*-alkanes from $C_3$ and $C_4$ grasses. Geochim. Cosmochim. Acta 70, 1172–1187.

Stenni, B., Masson-Delmotte, V., Johnsen, S., Jouzel, J., Longinelli, A., Monnin, E., Röthlisberger, R., Selmo, E., 2001. An oceanic cold reversal during the Last Deglaciation. Science 293, 2074–2077.

Street-Perrott, F.A., Perrott, R.A., 1990. Abrupt climate fluctuations in the tropics: the influence of Atlantic Ocean circulation. Nature 343, 607–612.

Talbot, M.R., Filippi, M.L., Jensen, N.B., Tiercelin, J.-J., 2007. An abrupt change in the African monsoon at the end of the Younger Dryas. Geochem. Geophys. Geosyst. 8, Q03005.

Talling, J.F., 1963. Origin of stratification in an Africa rift lake. Limnol. Oceanogr. 8, 68–78.

Tierney, J.E., Russell, J.M., Huang, Y., Sinninghe Damsté, J.S., Hopmans, E.C., Cohen, A.S., 2008. Northern Hemisphere controls on tropical southeast African climate during the past 60,000 years. Science 322, 252–255.

Tierney, J.E., Mayes, M.T., Meyer, N., Johnson, C., Swarzenski, P.W., Cohen, A.S., Russell, J.M., 2010. The unprecedented warming of Lake Tanganyika. Nat. Geosci. 3, 422–425.

Tierney, J.E., Russell, J.M., Sinninghe Damsté, J.S., Huang, Y., Verschuren, D., 2011. Late Quaternary behavior of the East African monsoon and the importance of the Congo Air Boundary. Quat. Sci. Rev. 30, 798–807.

Tierney, J.E., Smerdon, J.E., Anchukaitis, K.J., Seager, R., 2013. Multidecadal variability in East African hydroclimate controlled by the Indian Ocean. Nature 493, 389–392.

Tieszen, L.L., Senyimba, M.M., Imbamba, S.K., Troughton, J.H., 1979. The distribution of $C_3$ and $C_4$ grasses and carbon isotope discrimination along an altitudinal and moisture gradient in Kenya. Oecologia 37, 337–350.

Verschuren, D., Sinninghe Damste, J.S., Moernaut, J., Kristen, I., Blaauw, M., Fagot, M., Haug, G.H., 2009. Half-precessional dynamics of monsoon rainfall near the East African Equator. Nature 462, 637–641.

Vidal, L., Labeyrie, L., Cortijo, E., Arnold, M., Duplessy, J.C., Michel, E., Becqué, S., van Weering, T.C.E., 1997. Evidence for changes in the North Atlantic Deep Water linked to meltwater surges during the Heinrich events. Earth Planet. Sci. Lett. 146, 13–27.

Volkman, J.K., 2006. Lipid markers for marine organic matter. In: Volkman, J. (Ed.), Marine Organic Matter: Biomarkers, Isotopes and DNA. Springer, Berlin Heidelberg, pp. 27–70.

Waelbroeck, C., Labeyrie, L., Duplessy, J.C., Guiot, J., Labracherie, M., Leclaire, H., Duprat, J., 1998. Improving past sea surface temperature estimates based on planktonic fossil faunas. Paleoceanography 13, 272–283.

Weijer, W., De Ruijter, W.P.M., Sterl, A., Drijfhout, S.S., 2002. Response of the Atlantic overturning circulation to South Atlantic sources of buoyancy. Glob. Planet. Change 34, 293–311.

Weijers, J.W.H., Schefuß, E., Schouten, S., Sinninghe Damsté, J.S., 2007. Coupled thermal and hydrological evolution of tropical Africa over the last deglaciation. Science 315, 1701–1704.

Williams, M., Talbot, M., Aharon, P., Abdl Salaam, Y., Williams, F., Inge Brendeland, K., 2006. Abrupt return of the summer monsoon 15,000 years ago: new supporting evidence from the lower White Nile valley and Lake Albert. Quat. Sci. Rev. 25, 2651.

Zhang, R., Delworth, T.L., 2005. Simulated tropical response to a substantial weakening of the Atlantic thermohaline circulation. J. Clim. 18, 1853–1860.